

# Characterization of a Newly Developed Eco-friendly Phenol-paraPhenyleneDiAmine (P-pPDA) Coating for Outer Structure Applications in Aeronautical Industries

**Abhishek Chandramohan**

VPA Laboratory Private Limited,  
Chennai, Tamil Nadu, 600045, India

## Abstract

The protective coatings in metals enhances its physical properties against harm. In aeronautical industries, the structure is typically coated with paint at 100  $\mu\text{m}$ , which provides corrosion resistance. However, phenomenon such as lightning does not help the coating or paint against damage. In this work, a polymer i.e., P-pPDA is synthesized by introducing gold dusts in the final stages of preparation. The goal is to replace the use of paint with polymer coating to be more eco-friendly to the environment and also to form the coating in a way that the gold dusts helps dissipate the discharge from the lightning upon contact. Hence, materials characterization of the newly developed metal-matrix composite were performed to understand the interactions of the multilayers within the system.

*Keywords: Phenol-paraPhenyleneDiAmine (P-pPDA); Polymer coating; Materials characterization.*

## 1. Introduction

With the advancements in aeronautical industries, new solutions for high performance coatings i.e. better resistance to erosion, good electrical conductivity and flame retardant properties are on the rise. The synthesis of polymers, whose intrinsic properties are more efficient, has potential applications in the field of adhesives and paints. It has long been demanded for eco-friendly protective coatings to replace the non-degradable materials because the eco-friendly polymers has better thermal stability, resistance to chemical compounds and resistance to degradation in aggressive media.

Benzoxazine resins are gaining popularity due to its excellent properties such as compound stability and high glass transition temperature because these molecules are easy to synthesize. In addition, they experience low shrinkage during crosslinking mechanism because it is an aromatic compound. It is also possible to formulate different compounds with different precursors on benzoxazine monomers [1]. One such compound is P-pPDA and this work focuses on formulating a compound for thin film applications.

## 2. Synthesis of Composite

Part of the multilayers were prepared similar to the techniques demonstrated by Alexis Renaud et al. [2]. The composite (Fig. 1) contains an unclad Al 2024-T3 of 1 mm thickness that was anodized up to 3  $\mu\text{m}$  thickness by an electrolytic setup of sulfotartaric acid. The metal was anodized to create a rough surface for the polymer to bond mechanically. The anodic layer was then spin-coated with P-pPDA (Fig. 2) for 2  $\mu\text{m}$  thickness, where the P-pPDA compound was prepared from p-phenylenediamine, paraformaldehyde and phenol.

The low thicknesses were kept in order to maintain a strong interaction with the oxide layer and the polymer, which provides better adhesion. The aim of the polymer coating is to replace the use of paints in aeronautical industries to be more eco-friendly to the environment.

Followed by polymer coating, gold dusts were dispersed immediately on top to create a thin deposition. The motivation to introduce gold dusts is

that in case of lightning, the conductive properties of the gold helps dissipate the discharge upon contact. Finally, the composite was cured at room temperature.

Gold dusts
P-pPDA, e = 2 $\mu$ m
Anodic layer, e = 3 $\mu$ m
Unclad Al 2024 T3, e = 1 mm

**Fig. 1. Schematic of multilayers**

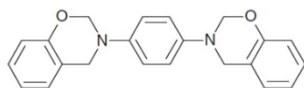


**Fig. 2. Synthesis of P-pPDA**

### 3. Materials Characterization

The inhomogeneity of P-pPDA was measured using a profilometer as  $\pm 100$  nm, which was due to spin-coating mechanism. The inhomogeneity influences surface characterization as well as contact parameters during experiment. The surface of each layers were observed under Field emission gun (FEG) Scanning electron microscope (SEM). The average size of pores were 12  $\mu$ m (Fig. 3) for anodic layer and 7.5  $\mu$ m (Fig. 4) for P-pPDA. It was observed that P-pPDA adapts the surface morphology of the anodic layer, which was due to its small thickness.

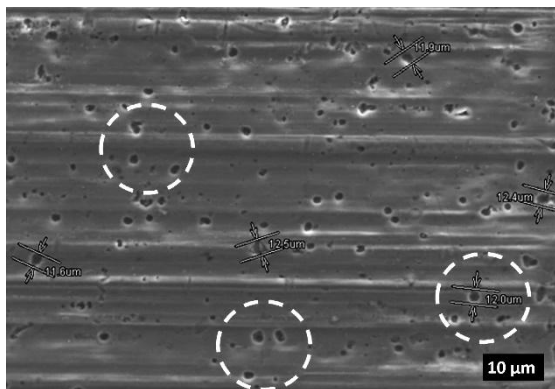


**Fig. 2. Porosity of plasma deposition under FIB SEM**

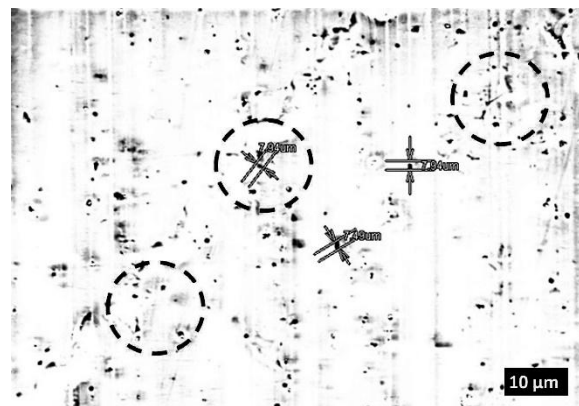


**Fig. 4. P-pPDA without gold dust**

Focused ion beam (FIB) cuts were made in order to observe the cross-sections of the multilayers. The size of the cuts were 6  $\mu$ m X 15  $\mu$ m X 0.1  $\mu$ m and were observed under transmission electron microscope (TEM). Al are well documented as crystalline and the dark spots (Fig. 5) signifies dislocations [3]. In case of anodic layer (Fig. 5), the amorphous properties were confirmed by hollow spots [4]. While a clear separation of layers is observed for oxide deposition and Al (Fig. 5), the rough surface in anodic layer provides good interactions with the polymer coating. Typical to polymers, P-pPDA is also amorphous, which is the clearly visible region (Fig. 6) and the transparency signifies the absence of any diffracting elements [5]. Upon a closer look at the interface (Fig. 6), there seems to be good bonding between the polymer and the rough surface of deposition.

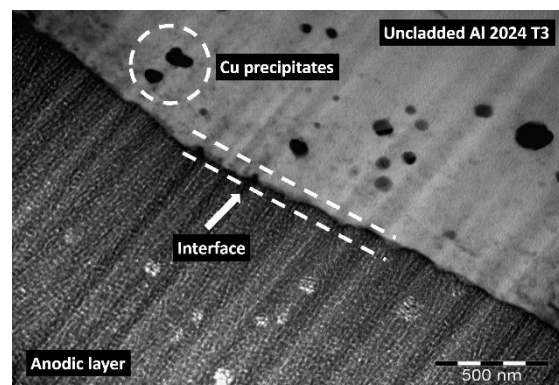


**Fig. 5. Anodic layer - Al, TEM**

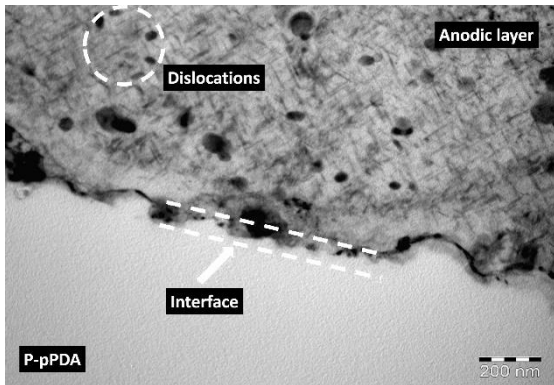


Fig. 6. P-pPDA – Anodic layer, TEM

The amorphous and crystalline properties of each layer were confirmed using x-ray diffraction (XRD) experiment (Fig. 7). In case of Al, diffraction (short peaks in plots) was observed, which signifies the crystalline structure of the material. For amorphous anodic layer, diffusion was observed i.e., curve [6]. As for the polymer layer, the long peaks signifies that the material is newly created in the database. The properties of all the layers were observed simultaneously because of the interaction zone. The interaction zone in XRD here was 25 mm in depth. However, the total thickness of the specimen synthesized was 1.005 mm. Hence, the information on all the layers can be seen. (It is to be noted that grazing incidence technique in XRD are mostly used to characterize the thin film since it does not have rotations [7].)

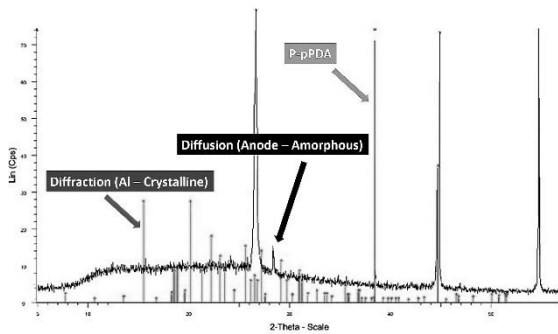


Fig. 7. XRD of composite

#### 4. Experiment

Experiments were performed on P-pPDA under nanoindentation using continuous stiffness measurements (CSM) technique. The model (Fig. 8, 9) consists of a spring of stiffness (S), a mass (m) and a dashpot (where D = damping coefficient). The principle of CSM is that upon an oscillating force, a corresponding response occurs. Unloading is eliminated in dynamic conditions, which provides accurate results from the experiment.

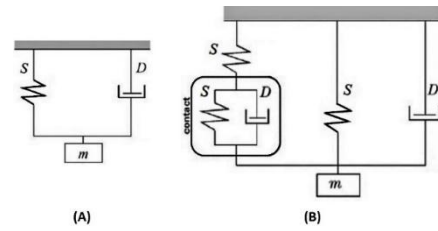


Fig. 8. (A). Model in free position and, (B). Model with indenter contact

The contact stiffness (S) is given by:

$$S_{contact} = \left[ \frac{P_o}{h_o} \cos\varphi + m\omega^2 \right]_{\text{coupled+ free position}} \quad (1)$$

$$P_o e^{i\omega t} = m\dot{h} + D\dot{h} + Sh \quad (2)$$

$$h = h_o e^{i(\omega t - \varphi)} \quad (3)$$

Where  $P_o$  = force amplitude,  $h_o$  = displacement amplitude,  $\varphi$  = phase angle,  $\omega$  = frequency and  $\dot{h}$  &  $\ddot{h}$  are the first and second order derivatives of depth = h, with respect to time = t.

#### 5. Results and Discussions

In the test environment, the maximum indentation depth ( $h_c$ ) reached without the influence of the anodic layer was 50%. S increases linearly with t (Fig. 9), typically exhibiting the property of a graded material. Here, S and E increases with increasing slope (Fig. 9, 10), which signifies that  $h_c$  calculated from rigid plastic theory with time-dependency is applicable to viscoelastic materials [8] i.e., polymer – P-pPDA. The hardness (H) for P-pPDA decreases with  $h_c$  initially (Fig. 10), which signifies a shallow indentation. The value of H over the range were measured as 0.6 GPa. Similarly, the modulus of elasticity (E) for P-pPDA over the range (Fig. 10) were measured as 10 GPa, which is a higher value for a polymer. However, a monomer compound of the same family i.e., mPDA, also has a higher value of 8.6 GPa [9]. This signifies that the PDA group has high stiffness.

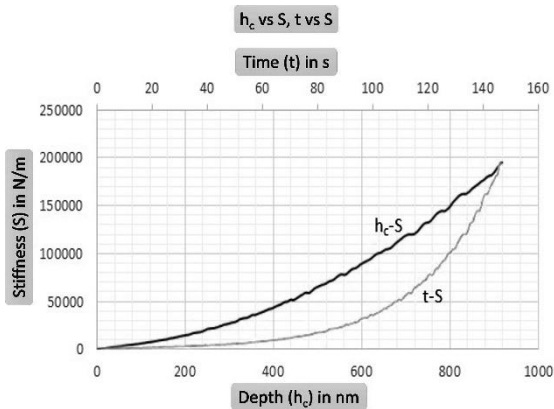


Fig. 9.  $h_c$  vs S, t vs S

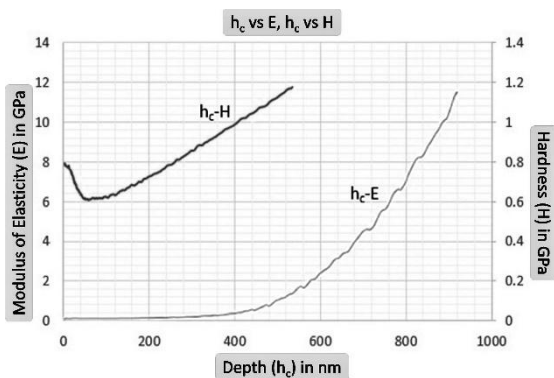


Fig. 10.  $h_c$  vs E,  $h_c$  vs H

## 6. Conclusion

A newly synthesized polymer coating was characterized in this work to understand its application in aeronautical industries as a replacement for paints. Initially, the polymer was characterized to observe how well it integrates with other compounds in the matrix. Experiments were then conducted to extract the values of H and E. An interesting theme of this work is the introduction of gold dusts in thin film polymer coating. The aim to have such a layer is to replace the use of paints in metals and also to dissipate the discharge from the lightning when it occurs i.e., protection against damage. The physical properties of the polymer is promising and studies on conductivity and failure mechanisms are prospects of this work.

## References

- [1] Delebecq E, Pascault J.P, Boutevin B, Ganachaud F, On the versatility of urethane/urea bonds : Reversibility, blocked isocyanate, and non-isocyanate polyurethane. *Chemical Reviews*, 113(1): 80-118, (2012).
- [2] Chattopadhyay D.K, Raju K.V.S.N, Structural engineering of polyurethane coatings for high performance applications. *Progress in Polymer Science*, 32(3): 352-418, (2007).
- [3] Mertens J, Baneton J, Ozkan A, Pospisilova E, Nysten B, Delcorte A, Reniers F, Atmospheric pressure plasma polymerization of organics: effect of the presence and position of double bonds on polymerization mechanisms, plasma stability and coating chemistry. *Thin Solid Films*, 671: 64-76, (2019).
- [4] Tryznowski M, Swiderska A, Zołek-Tryznowska Z, Gołofit T, Parzuchowski P.G, Facile route to multigram synthesis of environmentally friendly non-isocyanate polyurethanes. *Polymer*, 80: 228-236, (2015).
- [5] Rosner H, Molenat G, Nembach E, In situ TEM observations of dislocation processes in iron-aluminides with 25 and 30 at.% aluminium. *Materials Science and Engineering A*, 216: 169-177, (1996).
- [6] Paris P, Erdogan F, A critical analysis of crack propagation laws. *Journal of Basic Engineering*, 85(4): 528-534, (1963).
- [7] Arunakumara P.C, Dinesh P, Fatigue crack growth study in polymer matrix composites. *International journal of recent trends in engineering and research*, 2(5): 284-289, (2016).
- [8] Anderson T.L, *Fracture mechanics*, 4th Edition, CRC Press, Florida, 491-494, (2017).
- [9] Grasso M, Iorio A.D, Xu Y, Haritos G, Mohin M, Chen Y.K, An Analytical Model for the Identification of the Threshold of Stress Intensity Factor Range for Crack Growth. *Advances in Materials Science and Engineering*, 3: 1-13, (2017).
- [10] Mayer H, Schuller R, Fitzka M, Fatigue of 2024-T351 aluminium alloy at different load ratios up to  $10^{10}$  cycles. *International Journal of Fatigue*, 27: 113-119, (2013).